Hindawi Publishing Corporation
International Journal of Rotating Machinery
Volume 2008, Article ID 406809, 6 pages
doi:10.1155/2008/406809

Research Article

Thermal-Fluid Transport Phenomena between Twin Rotating Parallel Disks

Shuichi Torii[1] and Wen-Jei Yang[2]

[1] *Department of Mechanical System Engineering, Kumamoto University, Kumamoto 860-8555, Japan*
[2] *Mechanical Engineering and Applied Mechanics, University of Michigan, Ann Arbor, MI 48109, USA*

Correspondence should be addressed to Shuichi Torii, torii@mech.kumamoto-u.ac.jp

Received 11 April 2008; Accepted 5 June 2008

Recommended by Gerard Bois

This paper investigates thermal-fluid transport phenomena in laminar flow between twin rotating parallel disks from whose center a circular jet is impinged on the heated horizontal bottom disk surface. Emphasis is placed on the effects of the Reynolds number, rotation speed, and disk spacing on both the formations of velocity and thermal fields and the heat transfer rate along the heated wall surface. The governing equations are discretized by means of a finite-difference technique and are numerically solved to determine the distributions of velocity vector and fluid temperature under the appropriate boundary conditions. It is found from the study that (i) the recirculation zone which appears on the bottom disk moves along the outward direction with an increase in the Reynolds number, (ii) when the Reynolds number is increased, heat transfer performance is intensified over the whole disk surface and the minimum value of the heat transfer rate moves in the downstream direction, and (iii) the heat transfer rate is induced due to the disk rotation, whose effect becomes larger due to the upper disk rotation.

1. INTRODUCTION

The impinging gas and liquid jets are of general practical interest in many industrial fields, that is, in a wide variety of industrial processes for cooling and heating. Some industrial applications include the thermal treatment of metals, cooling of internal combustion engines, and thermal control of high-heat-dissipation electronic devices [1]. Both circular and planar liquid jets have attracted research attention. Polat et al. [2] reviewed the numerical analysis on laminar confined impinging jets of various configurations. In many practical engineering applications, the working fluid is impinged by a coaxial round jet for the purpose of controlling heat transfer performance on two- and three-dimensional channels (Ichimiya and Fukumoto [3]; Ichimiya and Yamada [4]).

Meanwhile, laminar heat transfer in corotating and stationary disk systems was studied theoretically and experimentally (Sim and Yang [5]; Mochizuki and Yang [6]; Mochizuki [7]; Prakash et al. [8]; Suryanarayana et al., [9]). Both numerical and experimental results indicated a substantial enhancement in heat transfer performance due to Coriolis, which is induced with an increase in the Reynolds number and/or the rotational speed. Radial outward flow between two coaxial disks occurs in a number of situations of engineering interest, including turbines, pumps, diffusions, rotating heat exchangers, disk brakes, trust bearings, and so forth. Owen [10, 11] reviewed the literature pertinent to fluid flow and heat transfer in rotating disk systems: the rotating disk systems are classified into the free disk, rotor-stator system (which are used to simulate turbine disks rotating near stationary casings) and rotating cavities (which are used to simulate corotating turbine disks). Mochizuki and Yang [6] investigated the momentum and heat transfer in radial flow through parallel disks including the entrance effect. They obtained the heat transfer and friction factors and at zero rotating speed and reported that the heat transfer performance is comparable to those of high-performance compact plate-fin surfaces of plain, louvered, and strip type, while the friction factor is substantially higher than those of the compact surface. Heat transfer and friction loss in multiple parallel disk assemblies were measured by Mochizuki et al. [12] with the aid of a modified single-blow transient test method. They obtained a schematic flow

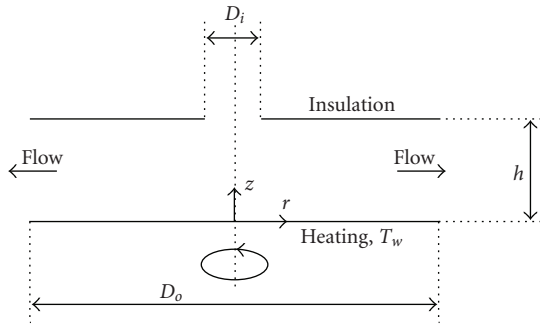

Figure 1: Schematic diagrams of two-dimensional channel wall impinged by planar dual jets and their coordinates.

map to determine the variation of flow patterns along the radial flow passage with the Reynolds number and disclosed three distinct mechanisms of convective enhancement, that is, the laminar-flow, "second" laminar-flow, and transition-turbulent flow enhancement. It was reported that the heat transfer performance based on the overall behavior throughout the entire flow channel exhibits characteristics of different convective mechanisms dependent on the flow regimes. Mochizuki and Yang [13, 14] carried out theoretical and experimental study on radial flow through two parallel disks with steady influx. It was found that (i) for lower Reynolds number Re, the slug flow at the inlet develops into a laminar profile toward the exit; (ii) as Re reaches a critical value, Re_c, vortexes separate alternately from both walls of the radial channel and stretch a distance downstream. Self-sustained flow oscillations are thus induced which diminish downstream and a laminar profile is grossly amplified and changed into a turbulent flow. However, due to continuous enlargement of the flow cross-sectional area in the radial direction, a reverse transition from turbulent to laminar flow takes place. However, to the authors' knowledge, there has been only a few information on thermal-fluid flow transport phenomena through rotating disk with circular impinging jet. To understand this transport phenomenon, it is necessary to investigate the corresponding fluid flows because detailed information on the heat and mass transfer is of great importance to many engineering applications.

The present study deals with thermal-fluid transport phenomena in laminar flow between a rotating bottom disk and a stationary or rotating upper disk from whose center a circular jet is impinged on the axially rotating heated horizontal bottom disk surface. Emphasis is placed on the effects of the Reynolds number, rotation speed and disk spacing on both the formations of velocity and thermal fields and the heat transfer rate along the heated wall surface. A numerical method is employed to determine the velocity and temperature profiles.

2. GOVERNING EQUATIONS AND NUMERICAL METHOD

Consider thermal-fluid transport phenomena in a pair of coaxial parallel disks of D_o in diameter in which the bottom wall rotating at an angular frequency Ω is heated at constant wall temperature T_w and is impinged from the circular pipe of D_i in diameter and the stationary upper wall is insulated. Here, the spacing between the disks is represented by h. The physical configuration of the coaxial disks with the impinging jet and the coordinate system of the flow are shown in Figure 1. The following assumptions are imposed in the formulation of the problem based on the characteristics of the flow: it is an incompressible laminar flow; fluid properties are constant because $T_w - T_{\mathrm{inlet}} < 5\,\mathrm{K}$; there is uniform velocity and uniform inlet fluid temperature T_{inlet} at the injection nozzle tip and negligible axial conduction (due to the high Peclet number). Then, the governing differential equations for mass, momentum, and energy can be expressed in the tensor formation as continuity equation:

$$\frac{\partial U_i}{\partial x_i} = 0, \tag{1}$$

momentum equation:

$$U_j \frac{\partial U_i}{\partial x_j} = -\frac{1}{\rho}\frac{\partial P}{\partial x_i} + \nu \frac{\partial}{\partial x_j}\left(\frac{\partial U_i}{\partial x_j}\right), \tag{2}$$

energy equation:

$$U_i \frac{\partial T}{\partial x_i} = a \frac{\partial}{\partial x_i}\left(\frac{\partial T}{\partial x_i}\right). \tag{3}$$

An isothermal laminar flow is assumed as the inlet condition. The boundary conditions in the stationary and rotating disks are specified as

$$\begin{aligned}
&U = V = 0, \quad W = W_w, \quad T = T_w, \quad \text{at bottom wall,}\\
&U = V = W = 0, \quad \text{or} \quad W = -W_w, \quad \frac{\partial T}{\partial z} = 0, \quad \text{at upper wall,}\\
&U = U_{\mathrm{in}}, \quad V = 0, \quad W = 0, \quad T = T_{\mathrm{inlet}}, \quad \text{at the impinging nozzle,}\\
&\frac{\partial U}{\partial r} = 0, \quad V = W = 0, \quad \frac{\partial T}{\partial r} = 0, \quad \text{at center } (r = 0),\\
&\frac{\partial U}{\partial r} = 0, \quad \frac{\partial V}{\partial r} = 0, \quad \frac{\partial W}{\partial r} = 0, \quad \frac{\partial T}{\partial r} = 0, \quad \text{at outlet, that is, } r = D_o/2.
\end{aligned} \tag{4}$$

A set of the governing equations is solved using the control-volume-based formulation of Patankar [15]. In this procedure, the domain is discretized by a series of control volumes, with each control volume containing a grid point. Each differential equation is expressed in an integral manner over the control volume, and profile approximations are made in each coordinate direction, leading to a system of algebraic equations that can be solved in an iterative manner. The semi-implicit method for pressure-linked equations (SIMPLEs) algorithm is employed to couple the pressure and velocity fields [15]. A staggered grid is considered such that the velocity components are located at the control

volume faces, whereas pressure and temperature are located at the centers of control volumes to avoid the velocity-pressure decoupling. A power law interpolation scheme is used to evaluate the values of variables at the control volume interfaces. The discretized equations are solved with a line-by-line and the TDMA (tridiagonal-matrix algorithm). The convergence criteria of the residuals of all equations are asssumed to be less than 10^{-5} of total inflow rates. Computation reveals only a slight difference when the grid system is properly changed from $50\times50\times20(r,\theta,z)$ to $100\times100\times40$, resulting in a grid-independent solution. Hence, a grid system of $50\times50\times20$ with uniformly distributed nodal points is employed here to also save computation time. Based on the dataset obtained here, visualization of the flow and thermal fields is carried out using a commercially available 2D graphics software tool.

The numerical computation was performed on a personal computer using air as the working fluid (Pr = 0.71). The parameters used in the present study are radial ratio $D_o/D_i = 4$, dimensionless disk height $h/D_i = 0.05\sim0.1$, Reynolds number Re = 300~2000, and rotational Reynolds number $\mathrm{Re}_t = 0\sim3000$. Note that calculation is focused in the vicinity of the impinging jet region in which the forced convection flow is dominant.

Simulations with grids of various degrees of coarseness, as mentioned earlier, were conducted to determine the required resolution for grid-independent solutions. Throughout the Reynolds number range considered here, the maximum error was estimated to be about ±2% by comparing the solutions on regular and fine grids with twice of the grid points.

3. RESULTS AND DISCUSSION

The effect of Reynolds number on the local Nusselt number along the bottom disk in the absence of rotation is depicted in Figures 2(a) and 2(b) for $h/D_i = 0.05$ and 0.10, respectively. One observes that (i) the local Nusselt number is increased over the whole heated surface with an increase in the Reynolds number, as seen in Figure 2(a), and (ii) the same trend appears in the case of the wider disk, but heat transfer performance is substantially lower than that in the narrow disk, as seen in Figure 2(b). These characteristics are in accordance with that reported by Ichimiya and Fukumoto [3]. The streamwise location of the minimum heat transfer coefficient moves in the downstream direction, as the Reynolds number is increased. This is caused due to the presence of the recirculation zone, as shown in the following figures. In other words, this zone moves along the outward direction with an increase in the Reynolds number. This behavior becomes clearer for the velocity and temperature fields. Figure 3, for $h/D_i = 0.05$, illustrates the velocity vector and isotherms in the $r-z$ cross-section of the dick. The corresponding results for $h/D_i = 0.10$ are depicted in Figure 4. Here, $\Theta = 1$ and 0 in Figures 3 and 4 correspond to the heated wall temperature and the fluid temperature at the injection nozzle tip, respectively. Notice that the velocity components are normalized by dividing it by the fluid velocity at the injection nozzle tip. It is observed

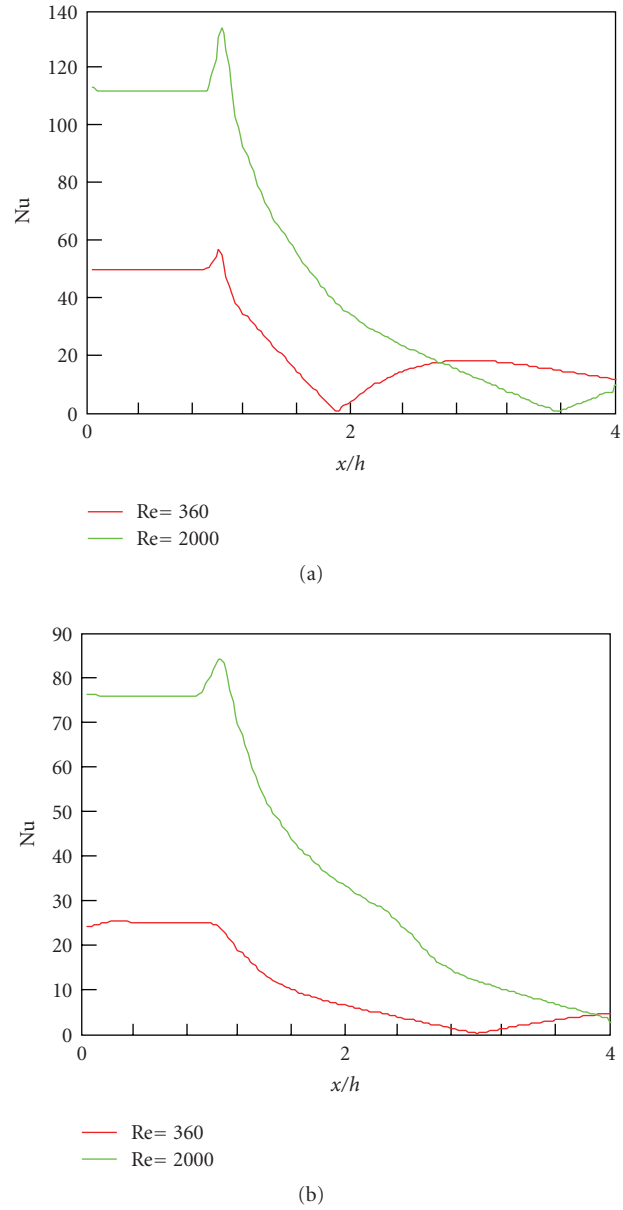

Figure 2: Local Nusselt Number on the Disk Surface, (a) $h/D_i = 0.05$ and (b) $h/D_i = 0.10$.

that a recirculation zone appears near the outlet of the injection nozzle and is extended with the increase of the channel width. Thermal boundary layer is developed along the heated wall and the temperature gradient at each axial location is intensified with a decrease in the channel width. This implies enhancement of heat transfer performance, as seen in Figure 2(a).

Figure 5, for Re = 2000, illustrates local Nusselt number Nu on the rotating disk surface with the rotating Reynolds number Re_t, as the parameter. (a) and (b) of Figure 5 correspond to numerical results at $h/D_i = 0.05$ and 0.10. Heat transfer performance for $h/D_i = 0.05$ becomes larger than that for $h/D_i = 0.10$. One observes that the Nusselt number is gradually diminished along the flow. For the

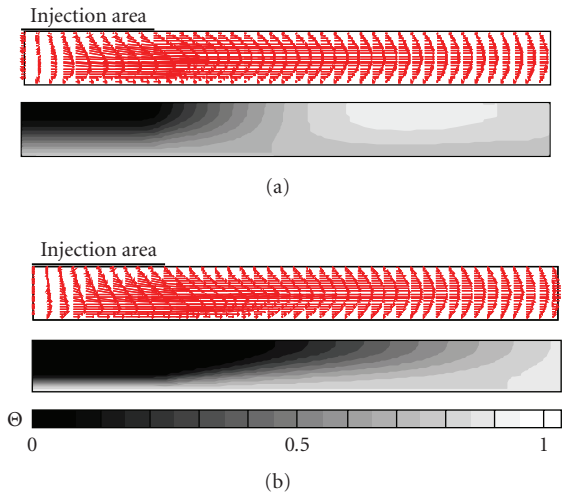

Figure 3: Velocity and temperature distributions in stationary disk at $h/D_i = 0.05$, (a) Re = 360, (b) Re = 2000.

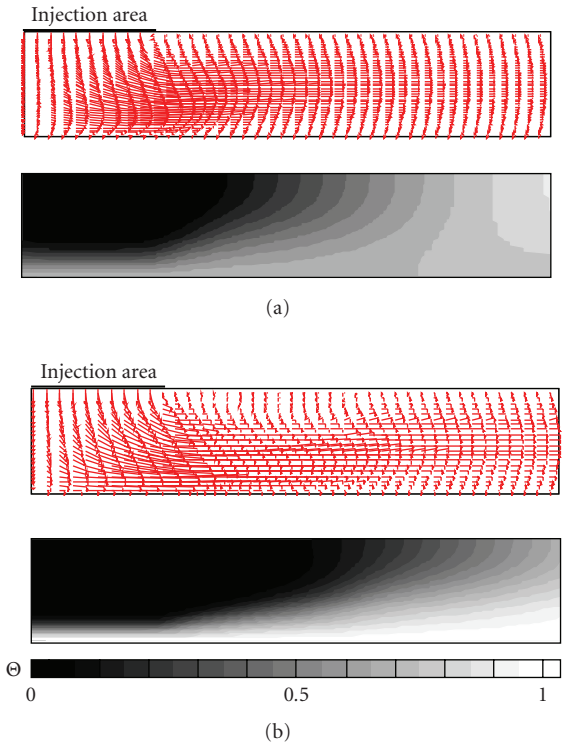

Figure 4: Velocity and temperature distributions in stationary disk at $h/D_i = 0.10$, (a) Re = 360, (b) Re = 2000.

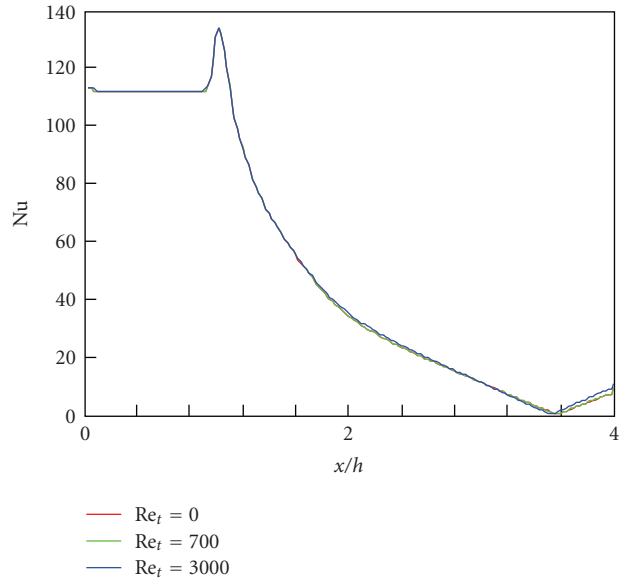

(a)

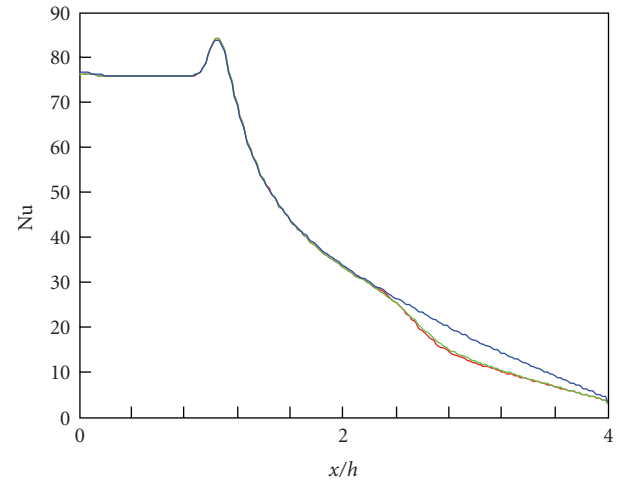

(b)

Figure 5: Local Nusselt Number on the Rotating Disk Surface for Re = 2000, (a) $h/D_i = 0.05$ and (b) $h/D_i = 0.10$.

narrow channel, there is no effect of disk rotation on heat transfer rate on its plate. On the contrary, the heat transfer rate is intensified by the disk rotation for the channel with the wide distance, as seen in Figure 5(b). The corresponding numerical results in the $r - z$ cross-section of the disk are illustrated in Figures 6 and 7 at $h/D_i = 0.05$ and 0.10, respectively. (a) and (b) in each figure correspond to the results of the velocity and thermal distributions, respectively. It is observed that the velocity and thermal fields in rotating disk, for $h/D_i = 0.05$, are the same as that in the stationary disk, while the corresponding fields for $h/D_i = 0.10$ are affected by the disk rotation, and the recirculation zone appears in the outlet of the rotating disk, resulting in a substantial deformation of the velocity and thermal fields. The presence of the recirculation zone induces the temperature gradient near the heated wall at the outlet of the disk, resulting in an increase of heat transfer performance, as seen in Figure 5(b). Thus, the effect of disk rotation on heat transfer performance is found to occur in the wider disk spacing. This trend became larger in the lower Reynolds number region (not shown).

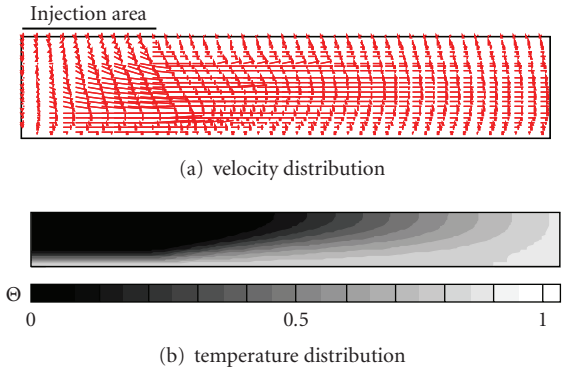

FIGURE 6: Velocity and temperature distributions in rotating disk at $h/D_i = 0.05$, Re = 2000 and $\mathrm{Re}_t = 2000$.

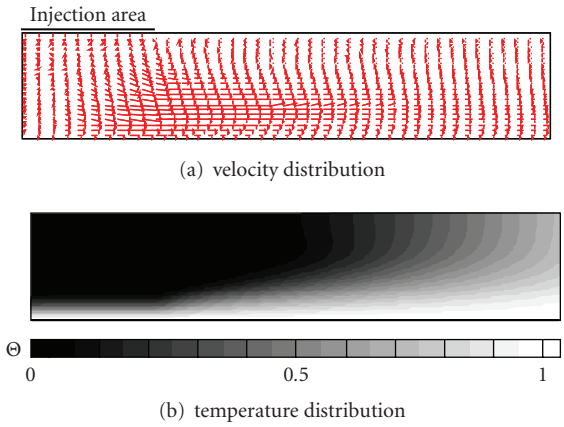

FIGURE 7: Velocity and temperature distributions in rotating disk at $h/D_i = 0.10$, Re = 2000 and $\mathrm{Re}_t = 2000$.

Next task is to study the effect of upper wall rotation on heat transfer rate and thermal and velocity fields. The local Nusselt number for $h/D_i = 0.1$ and Re = 360 is depicted in Figure 8 in the same form as Figure 5. One observes that when the upper and lower walls are simultaneously rotated in the opposite direction, the Nusselt number is intensified along the wall, particularly near the impinging region. The drastic enhancement of heat transfer performance becomes clearer in velocity and thermal fields. The corresponding numerical results in the $r - z$ cross-section of the disk are illustrated in Figures 9(a) and 9(b) in each figure correspond to the results of the velocity and thermal distributions, respectively. It is observed that the velocity in the vicinity of in rotating disk walls is increased along the exit due to the opposite flow in the center region of the parallel disk, resulting in an amplification of temperature gradient near the wall.

4. SUMMARY

Numerical simulation has been employed to investigate thermal-fluid transport phenomena in laminar flow between a rotating bottom disk and a stationary or rotating upper

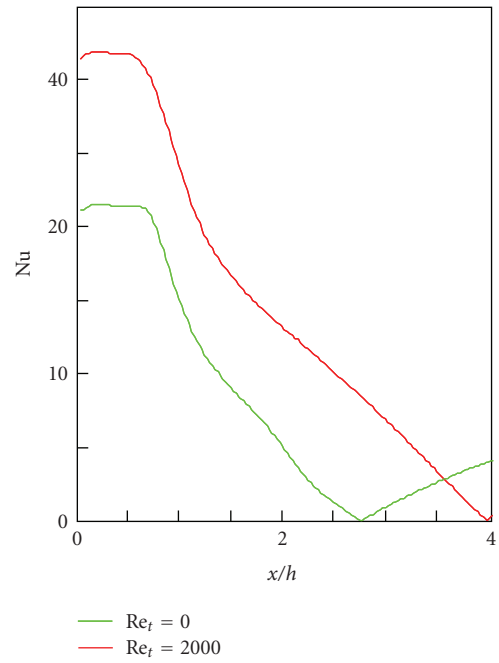

FIGURE 8: Local Nusselt Number on the rotating disk surface for Re = 360 and $h/D_i = 0.1$.

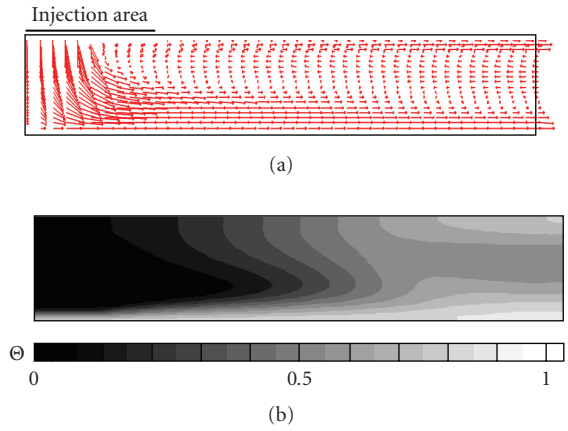

FIGURE 9: Velocity and temperature distributions in rotating disks for $h/D_i = 0.10$ and Re = 360.

disk, from whose center a circular jet is impinged on the axially rotating heated horizontal bottom disk surface. Consideration is given to the effects of the Reynolds number, rotation speed, and disk spacing on both the formations of velocity and thermal fields and the heat transfer rate along the heated bottom surface. The results are summarized as follows.

(1) The recirculation zone appears on the stationary disk. This zone moves along the outward direction with an increase in the Reynolds number.

(2) The heat transfer rate approaches the minimum rate due to the presence of the recirculation zone. When the Reynolds number is increased, heat transfer performance is

intensified over the whole disk surface and the streamwise location of the minimum heat transfer rate moves in the downstream direction. This trend yields for the channels with different width.

(3) The heat transfer rate is induced due to the disk rotation, whose effect becomes larger in the wider disk spacing.

(4) Further enhancement heat transfer causes when the upper and lower walls are simultaneously rotated in the opposite direction.

NOMENCLATURE

a: Thermal diffusivity, m^2/s
D_i: Injection inner nozzle diameter, m
D_o: Disk diameter, m
h: Disk spacing, m
L: Channel length—disk radius, m
Nu: Nusselt number, $\alpha D_i/\lambda$
P: Time-averaged pressure, Pa
r: Radial direction
Re: Reynolds number, $U_i D_i/\nu$
Re_t: Rotational Reynolds number, $\Omega D_i^2/\nu$
T: Temperature, K
T_{inlet}: Inlet temperature of circular pipe, K
T_w: Wall temperature, K
U, V: Time-averaged velocity components in z and r directions, respectively, m/s
U_i: Axial mean velocity over the injection nozzle or velocity, m/s
W_w: Tangential velocity at bottom wall, m/s
x_i: Coordinate, m
r, z: Radial and axial direction, respectively, m

GREEK LETTERS

α: Heat transfer coefficient at heated bottom wall, $W/m^2/K$, $\alpha = \lambda(\partial T/\partial y)|_{z=0}/(T_w - T_{\mathrm{inlet}})$
ν: Molecular viscosity, m^2/s
p: Density of fluid, kg/m^3
λ: Thermal conductivity, W/m/K
Ω: Angular frequency
θ: Tangential direction
Θ: Dimensionless temperature $\Theta = (T - T_{\mathrm{inlet}})/(T_w - T_{\mathrm{inlet}})$

SUBSCRIPTS

W: Wall
inlet: Inlet of circular pipe

REFERENCES

[1] B. W. Webb and C. F. Ma, "Single-phase liquid jet impingement heat transfer," in *Advances in Heat Transfer, Vol. 26*, J. P. Hartnett, T. F. Irvine, Y. I. Cho, and G. A. Greene, Eds., pp. 105–217, Academic Press, New York, NY, USA, 1995.

[2] S. Polat, B. Huang, A. S. Mujumdar, and W. J. W. Douglas, "Numerical flow and heat transfer under impinging jets: a review," in *Annual Review of Numerical Fluid Mechanics and Heat Transfer, Vol. 2*, C. L. Tine and T. C. Chawla, Eds., pp. 157–197, Hemisphere, Washington, DC, USA, 1989.

[3] K. Ichimiya and H. Fukumoto, "Effect of a nozzle shape on annular impingement heat transfer," in *Proceedings of the 33rd National Heat Transfer Symposium*, vol. 2, pp. 387–388, Niigata, Japan, May 1996.

[4] K. Ichimiya and Y. Yamada, "Three-dimensional characteristics of heat transfer and flow and visualization on a single circular laminar impinging jet in comparatively narrow space," *Transaction of the Visualization Society of Japan*, vol. 20, no. 78, pp. 250–255, 2000.

[5] Y. S. Sim and W.-J. Yang, "Numerical study on heat transfer in laminar flow through co-rotating parallel disks," *International Journal of Heat and Mass Transfer*, vol. 27, no. 11, pp. 1963–1970, 1984.

[6] S. Mochizuki and W.-J. Yang, "Heat transfer and friction loss in laminar radial flows through rotating annular disks," *Journal of Heat Transfer*, vol. 103, no. 2, pp. 212–217, 1981.

[7] S. Mochizuki, "Unsteady flow phenomena and heat transfer in rotating-disk systems," in *Transport Phenomena in Thermal Engineering, Vol. 2*, Begell House, New York, NY, USA, 1993.

[8] C. Prakash, U. S. Powle, and N. V. Suryanarayana, "Analysis of laminar flow and heat transfer between a stationary and a rotating disk," *AIAA Journal*, vol. 23, no. 11, pp. 1666–1667, 1985.

[9] N. V. Suryanarayana, T. Scofield, and R. E. Kleiss, "Heat transfer to a fluid in radial, outward flow between two coaxial stationary or corotating disks," *Journal of Heat Transfer*, vol. 105, no. 3, pp. 519–526, 1983.

[10] J. M. Owen, "Fluid flow and heat transfer in rotating disc system," in *Proceedings of the 14th Symposium of the International Centre for Heat and Mass Transfer (ICHMT '82)*, Dubrovnik, Yugoslavia, September 1982.

[11] J. M. Owen, "Fluid flow and heat transfer in rotating disk systems," in *Heat and Mass Transfer in Rotating Machinery*, D. E. Metzger and N. H. Afgan, Eds., Hemisphere, Washington, DC, USA, 1984.

[12] S. Mochizuki, W.-J. Yang, Y. Yagi, and M. Ueno, "Heat transfer mechanisms and performance in multiple parallel disk assemblies," *Journal of Heat Transfer*, vol. 105, no. 3, pp. 598–604, 1983.

[13] S. Mochizuki and W.-J. Yang, "Three mechanisms of convective enhancement in stationary disk systems," *Journal of Heat Transfer*, vol. 108, no. 4, pp. 978–980, 1986.

[14] S. Mochizuki and W.-J. Yang, "Flow friction on co-rotating parallel-disk assemblies with forced through-flow," *Experiments in Fluids*, vol. 4, no. 1, pp. 56–60, 1986.

[15] S. V. Patankar, *Numerical Heat Transfer and Fluid Flow*, Hemisphere, Washington, DC, USA, 1980.